Check for updates

MntP and YiiP Contribute to Manganese Efflux in *Salmonella enterica* Serovar Typhimurium under Conditions of Manganese Overload and Nitrosative Stress

Annie Ouyang,[a] Kendall M. Gasner,[a] Stephanie L. Neville,[b] Christopher A. McDevitt,[b] Elaine R. Frawley[a]

[a]Rhodes College Biology Department, Memphis, Tennessee, USA
[b]Department of Microbiology and Immunology, The Peter Doherty Institute for Infection and Immunity, The University of Melbourne, Victoria, Australia

ABSTRACT The divalent transition metal cation manganese is important for protein function, particularly under conditions of iron limitation, nitrosative stress, and oxidative stress, but can mediate substantial toxicity in excess. *Salmonella enterica* serovar Typhimurium possesses multiple manganese importers, but the pathways for manganese efflux remain poorly defined. The *S.* Typhimurium ATCC 14028s genome was analyzed for putative manganese export pathways, which identified a previously uncharacterized homologue of the *Escherichia coli* manganese exporter *mntP*, *stm1834,* and two cation diffusion facilitator family transporters, *zitB* (*stm0758*) and *yiiP* (*stm4061*). Manganese acquisition by *S.* Typhimurium has been shown to occur in response to nitric oxide, an important chemical mediator of the mammalian innate immune response. However, cellular manganese can rapidly return to prechallenge levels, strongly suggesting that one or more *S.* Typhimurium exporters may contribute to this process. Here, we report that *mntP* and *yiiP* contribute to manganese resistance and export in *S.* Typhimurium. YiiP, also known as FieF, has previously been associated with zinc and iron transport, although its physiological role remains ambiguous due to a lack of zinc-sensitive phenotypes in *yiiP* mutant strains of *S.* Typhimurium and *E. coli*. We report that *S.* Typhimurium Δ*mntP* Δ*yiiP* mutants are exquisitely sensitive to manganese and show that both YiiP and MntP contribute to manganese efflux following nitric oxide exposure.

IMPORTANCE Transition metal cations are required for the function of many proteins but can mediate toxicity when present in excess. Identifying transporters that facilitate metal ion export, the conditions under which they are expressed, and the role they play in bacterial physiology is an evolving area of interest for environmental and pathogenic organisms. Determining the native targets of metal transporters has proved challenging since bioinformatic predictions, *in vitro* transport data, and mutant phenotypes do not always agree. This work identifies two transporters that mediate manganese efflux from the Gram-negative pathogen *Salmonella enterica* serovar Typhimurium in response to manganese overload and nitric oxide stress. While homologues of MntP have been characterized previously, this is the first observation of YiiP contributing to manganese export.

KEYWORDS *Salmonella*, efflux pumps, manganese, metal ion homeostasis, nitric oxide

Metal cofactors are important to the function of many proteins, including nearly half of all enzymes (1, 2). *Salmonella enterica* serovar Typhimurium (*S.* Typhimurium), like many bacteria, possesses a variety of high-affinity import systems for divalent cations including magnesium, iron, zinc, and manganese (3–9). Import of manganese, which is not required for growth of *S.* Typhimurium under standard laboratory conditions, is important for growth under conditions of oxidative stress, nitrosative stress, and iron limitation, as well as within host environments (8, 10–14).

While manganese is beneficial under a variety of stress conditions, it can be toxic at elevated concentrations. Studies in *Escherichia coli* have shown that excess intracellular

manganese inhibits heme biosynthesis while chronic manganese stress ultimately leads to iron depletion and impaired formation of Fe-S cluster proteins (15, 16). Together, these effects can result in inhibition of energy-generating and biosynthetic pathways. In *Bacillus subtilis*, which requires manganese for growth, excess manganese has been associated with impaired function of the cytochrome aa_3 heme-copper menaquinol oxidase (QoxABCD) of the electron transport chain (17). Therefore, while increased cellular manganese may benefit bacteria when challenged with a specific physiological or chemical stress, efflux of manganese may be necessary upon alleviation of the aforementioned stress.

Three types of manganese efflux systems have been identified in prokaryotes to date. Transporters from the cation diffusion facilitator (CDF) family are widely prevalent among prokaryotic species with family members implicated in transport of zinc, cadmium, cobalt, nickel and manganese, depending on the sequence motifs present in metal binding regions (18). The prokaryotic CDF manganese exporter MntE was first identified in *Streptococcus pneumoniae* and has since been studied in *Staphylococcus aureus*, *Enterococcus faecalis*, and *Streptococcus pyogenes* (19–22). *B. subtilis* relies on two CDF family transporters for manganese efflux with MneP functioning as the primary exporter and MneS playing a secondary role (23). P_{1B}-ATPases have been shown to export a range of transition metal ions, with manganese export first established for CtpC from *Mycobacterium tuberculosis* (24). MntP, which lacks homology to other established classes of manganese exporters, was first characterized in *Xanthomonas oryzae*, *E. coli*, and *Neisseria meningitidis* (as MntX) (25–27). This architecturally distinct transporter has since been shown to have orthologs in additional species.

Previously, we showed that manganese acquisition by MntH, SitABCD, and ZupT is important for *S*. Typhimurium nitrosative stress resistance. Furthermore, total cellular manganese was restored to prechallenge levels following the resolution of the stress (14). In this study, we sought to identify and characterize *S*. Typhimurium efflux systems that contribute to manganese homeostasis in response to stress. We show that orthologs of the *E. coli* transporters MntP and YiiP protect *S*. Typhimurium against manganese intoxication and mediate manganese efflux during the late-stage response to nitrosative stress.

RESULTS

STM1834 (MntP) protects *S*. Typhimurium against excess manganese. *E. coli* and *S*. Typhimurium share similar genetic sequences at many loci, so the *S*. Typhimurium genome was searched for proteins with homology to MntP from *E. coli*. One match, at locus *stm1834* (Fig. 1A), was identified with 91% identity and 96% similarity (over 188 amino acids) to *E. coli* MntP. To determine the function of the putative *S*. Typhimurium *mntP* ortholog, a deletion mutant was generated. The mutant was then grown in the presence of 0.5 mM $MnSO_4$ and the phenotype compared to the wild-type parental strain. The *S*. Typhimurium Δ*mntP* strain was delayed for growth in excess manganese compared to the wild-type (Fig. 1B). Constitutive expression of *S*. Typhimurium *mntP* from a low-copy-number plasmid (pMntP) complemented the growth defect of a Δ*mntP* mutant (Fig. 1C). Consistent with the growth phenotype data, spot plate assays on manganese supplemented media showed that the *S*. Typhimurium Δ*mntP* strain had decreased growth on 0.5 mM $MnSO_4$ and decreased survival on 1 mM $MnSO_4$, while expression of *mntP* complemented these phenotypes (Fig. 1D). Taken together, these data are consistent with previous studies of MntP function in *E. coli* and suggest that *stm1834* encodes a manganese exporter homologous to *E. coli* MntP (26).

MntP is not solely responsible for manganese efflux following NO· treatment. To determine if manganese export by MntP is responsible for returning cellular manganese levels to pretreatment levels following NO· exposure, we compared the phenotypes of wild-type and Δ*mntP* *S*. Typhimurium by inductively coupled plasma-mass spectrometry (ICP-MS). Here, we used conditions defined in our prior studies of *S*. Typhimurium wherein the application of NO· stress alters metal homeostasis and induces manganese accumulation (14, 28). Accordingly, cultures were treated with 2 mM diethylamine NONOate (DEANO), a fast-release NO· donor, and the cellular manganese content was monitored over the course of 60 min. Consistent with prior observations, manganese levels increased by 30 min posttreatment and
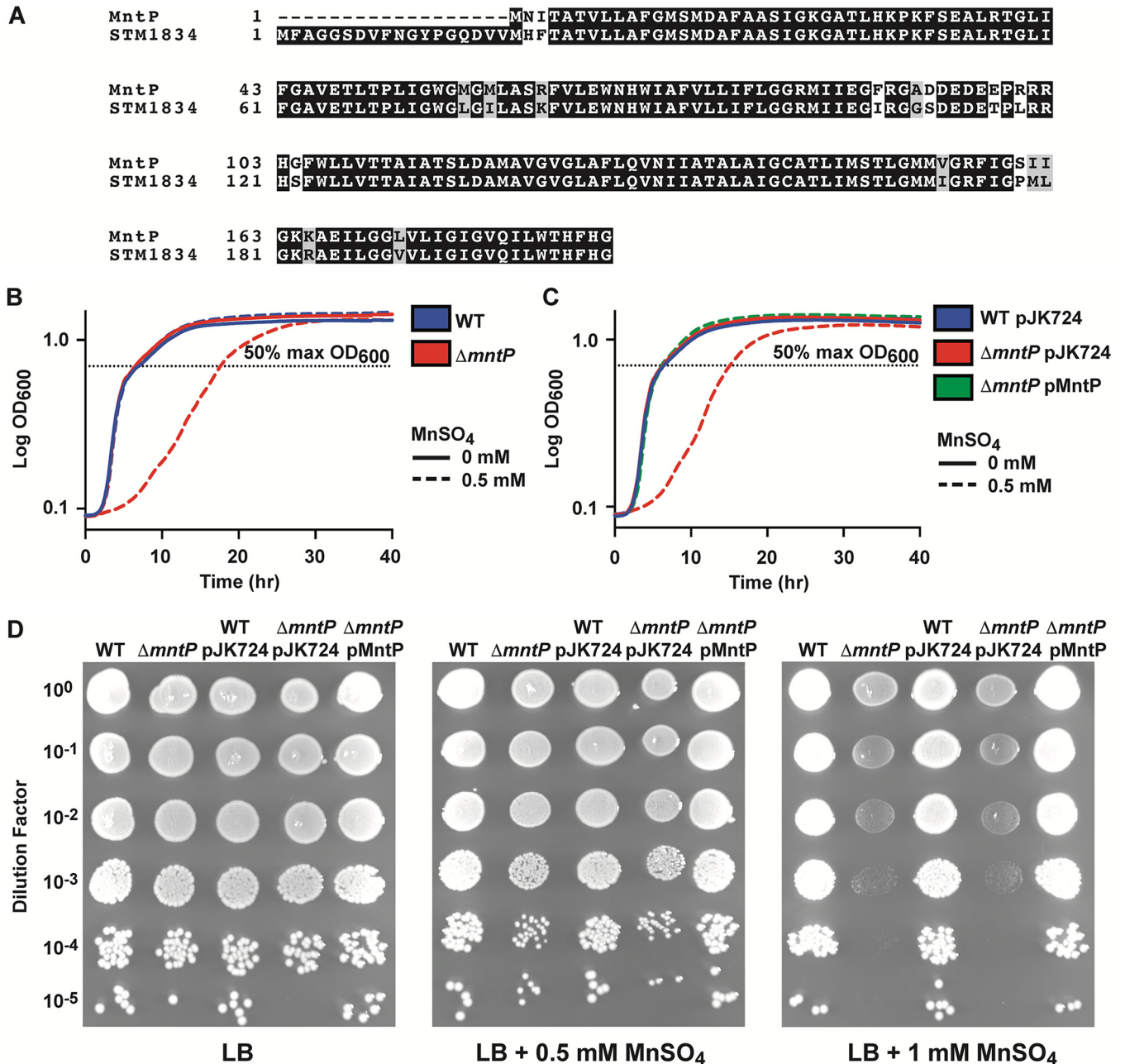
FIG 1 Deletion of the putative efflux transporter *stm1834* (*mntP*) delays growth of *S.* Typhimurium in 0.5 mM manganese. (A) Amino acid sequence alignment of *E. coli* MG1655 MntP (B3915) with *S.* Typhimurium STM1834. Identical residues are shown in black, while similar residues are shown in gray. (B) Growth phenotypes of *S.* Typhimurium wild-type (WT) and Δ*mntP* strains in LB with or without 0.5 mM $MnSO_4$ supplementation. The Δ*mntP* strain was delayed exiting lag phase relative to WT in the presence of 0.5 mM $MnSO_4$ ($P < 0.001$). (C) Growth phenotypes of *S.* Typhimurium empty vector strains WT pJK724 and Δ*mntP* pJK724 compared to plasmid-based complementation strain Δ*mntP* pMntP. In 0.5 mM $MnSO_4$ the Δ*mntP* pJK724 strain was delayed exiting lag phase compared to both WT pJK724 and Δ*mntP* pMntP ($P < 0.001$). Data for (B) and (C) are the mean of 4 independent experiments. Statistical significance of differences between strains was determined by the time (hr) to reach 50% maximum growth (OD_{600}; dashed line) by unpaired two-tailed *t* test. (D) Growth of strains from (B) and (C) assessed using spot assays. Dilutions of OD_{600} = 0.3 cultures were spotted onto LB agar with and without $MnSO_4$ supplementation. A representative spot assay for each condition is shown, selected from 3 independent biological replicates.

then returned to pretreatment levels by 60 min (Fig. 2) (14). Notably, manganese levels in the Δ*mntP* strain were not significantly different than in the wild-type at any time. These data indicate either that manganese efflux does not occur via MntP following NO· treatment or that, in the absence of *mntP*, manganese efflux occurs via another transporter in *S.* Typhimurium.

YiiP expression enhances zinc toxicity in *S.* Typhimurium. Since the *S.* Typhimurium genome contained only one MntP homologue, the genome was next searched for proteins with homology to the CDF family manganese transporter MntE. Two *S.* Typhimurium
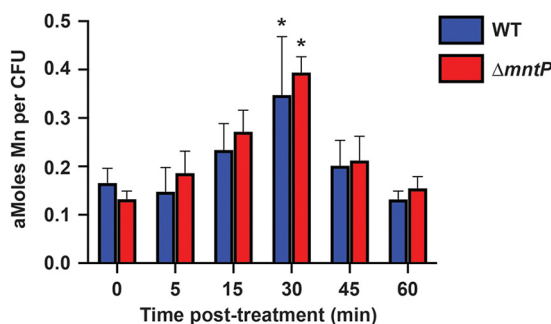
FIG 2 Intracellular manganese levels are not significantly different in Δ*mntP S.* Typhimurium compared to the wild-type following NO· treatment. Total cellular manganese in *S.* Typhimurium wild-type (WT) and Δ*mntP* strains determined by ICP-MS following addition of 2 mM DEANO. Manganese levels were significantly elevated (*) for WT ($P = 0.026$) and Δ*mntP* ($P < 0.001$) at 30 min posttreatment compared to 0 min. At no time were manganese levels in the Δ*mntP* strain significantly different from WT. Data are the mean (± standard deviation) of 3 independent experiments. Statistical significance of differences between strains and across time points for each strain was determined by unpaired two-tailed *t* test.

proteins were observed to have similarity to *S. pneumoniae* MntE. YiiP (STM4061) had the greatest similarity with 28% identity and 50% similarity over 264 amino acids. In addition to homology with MntE, YiiP also shares homology (26% identity and 51% similarity over 183 amino acids) with CzcD, a well-studied CDF family zinc transporter (Fig. 3A). ZitB (STM0758), a zinc transporter in *E. coli* and *S.* Typhimurium, had 20% identity and 48% similarity over 201 amino acids compared to *S. pneumoniae* MntE (28, 29).

E. coli YiiP, also known as FieF, was first reported to serve as an iron efflux transporter. Subsequent *in vitro* studies showed that YiiP also had the ability to interact with zinc ions, although its physiological contribution to zinc homeostasis remains to be defined (30–33). Three metal binding regions, the A-site, B-site, and C-site (comprised of C1 and C2 plus a linker) have been identified based on the *E. coli* YiiP crystal structure (31, 32, 34). The A-site has been established as the primary motif determining metal selectivity (34, 35). *S. pneumoniae* MntE has an ND-DD A-site motif, but DD-DD A-site motifs are also common in manganese exporting CDF proteins (36). By contrast, the zinc exporting CDF from *S. pneumoniae*, CzcD, has an HD-HD motif, which is the most common motif in CDF family zinc transporters (36). *S.* Typhimurium YiiP has a DD-HD A-site motif, which precludes bioinformatic prediction of the native ligand but is suggestive of the potential to export ions other than zinc.

Zinc sensitivity phenotypes have not been observed for *S.* Typhimurium or *E. coli* strains with *yiiP* deleted alone or in combination with other known zinc exporters (28, 29, 37). However, these studies could have failed to detect zinc sensitivity phenotypes if *yiiP* was not expressed under the conditions tested. To address this, we expressed *yiiP* constitutively from a low-copy-number plasmid (pYiiP) in the *S.* Typhimurium Δ*zntA* Δ*zitB* background to ascertain whether this could decrease the zinc sensitivity of this mutant strain. We observed that the Δ*zntA* Δ*zitB* strain was delayed for growth in the presence of 0.125 mM ZnSO₄ compared to the wild-type. Expression of *yiiP* in the Δ*zntA* Δ*zitB* genetic background abrogated bacterial growth (Fig. 3B). Notably, expression of *mntP* elicited a similar phenotype in the Δ*zntA* Δ*zitB* background (Fig. 3C). Spot assays revealed that expression of either YiiP or MntP in the Δ*zntA* Δ*zitB* genetic background led to decreased survival in the presence of 0.0625 mM ZnSO₄ and little to no survival on plates with 0.125 mM ZnSO₄ (Fig. 3D). These data indicate that YiiP does not facilitate zinc export. It therefore follows that the increased sensitivity of the *yiiP*-expressing Δ*zntA* Δ*zitB* strain suggests that YiiP may export a different metal ion that results in enhanced susceptibility to zinc intoxication.

Metal availability results in altered expression of *mntP* but not *yiiP*. We next measured *yiiP* expression under conditions of metal limitation, metal stress, and NO· challenge compared to *mntP*. In the presence of general divalent cation chelator ethylenediaminetetraacetic acid (EDTA), expression of neither *mntP* nor *yiiP* was significantly altered (Fig. 4A). In response to metal stress, *mntP* was upregulated when the medium was supplemented with
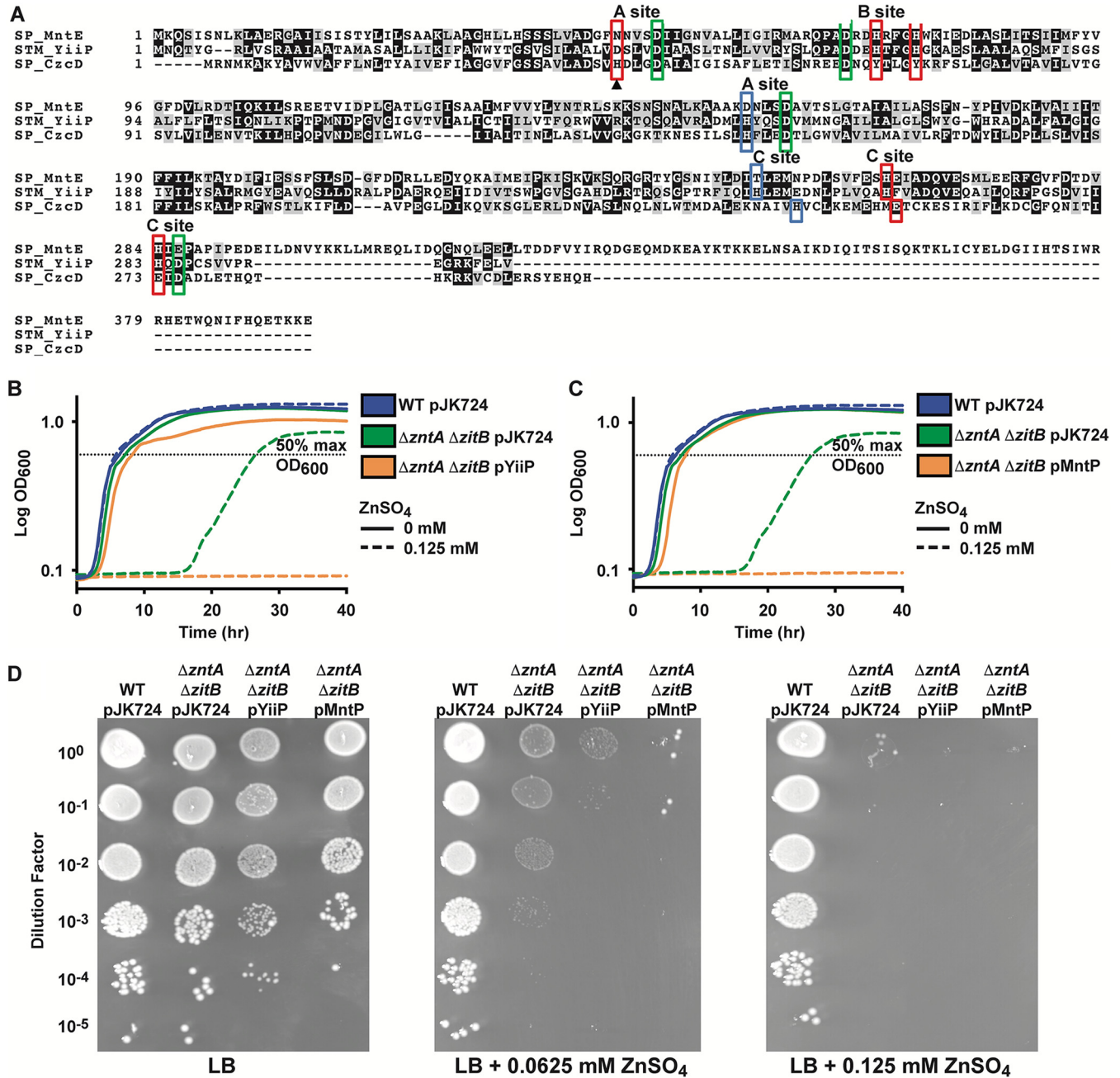
FIG 3 Expression of YiiP, a protein with homology to MntE and CzcD, enhances zinc sensitivity of an *S.* Typhimurium zinc efflux mutant strain. (A) Alignment of amino acid sequences for *S.* Typhimurium YiiP (STM_YiiP) and the related CDF proteins *S. pneumoniae* MntE (SP_MntE, SP_1552) and *S. pneumoniae* CzcD (SP_CzcD, SP_1857). Identical residues are shown in black, while similar residues are shown in gray. Metal-binding sites from the YiiP crystal structure (PDB ID: 2QFI) are shown. Ligands shared by all proteins are in green boxes. Red boxes denote ligands shared between YiiP and MntE. Blue boxes denote ligands shared between YiiP and CzcD. Boxes are staggered where the amino acid sequence alignment did not match previously assigned locations for two CzcD C-site residues. (B) Growth of *S.* Typhimurium wild-type (WT) pJK724, $\Delta zntA$ $\Delta zitB$ pJK724, and $\Delta zntA$ $\Delta zitB$ pYiiP strains in LB with or without 0.125 mM $ZnSO_4$ supplementation. The $\Delta zntA$ $\Delta zitB$ pJK724 strain was delayed exiting lag phase compared to WT pJK724 in 0.125 mM $ZnSO_4$ ($P < 0.001$), while the $\Delta zntA$ $\Delta zitB$ pYiiP strain failed to grow. (C) Growth of *S.* Typhimurium wild-type (WT) pJK724, $\Delta zntA$ $\Delta zitB$ pJK724, and $\Delta zntA$ $\Delta zitB$ pMntP strains in LB with or without 0.125 mM $ZnSO_4$ supplementation. Data for the growth curves (B) and (C) are the mean of 3 independent experiments. Statistical significance of the difference between the mutant strains and the wild-type was determined using the time (hr) to reach 50% maximum growth (OD_{600}; dashed line) and an unpaired two-tailed t test. (D) Growth of strains from (B) and (C) were assessed by spot assays. Dilutions of $OD_{600} = 0.3$ cultures were spotted onto LB agar supplemented with $ZnSO_4$ as shown. Zinc efflux mutants expressing YiiP or MntP show decreased survival in the presence of $ZnSO_4$. A representative spot assay for each condition is shown, selected from 3 independent replicates.

0.5 mM iron or manganese, but not zinc (Fig. 4B). By contrast, *yiiP* expression did not change in response to iron, manganese, or zinc (Fig. 4B), which also differs from observations of the orthologous gene from *E. coli* (29, 30). Expression of neither *mntP* nor *yiiP* was significantly altered at any time following treatment with 2 mM DEANO (Fig. 4C).
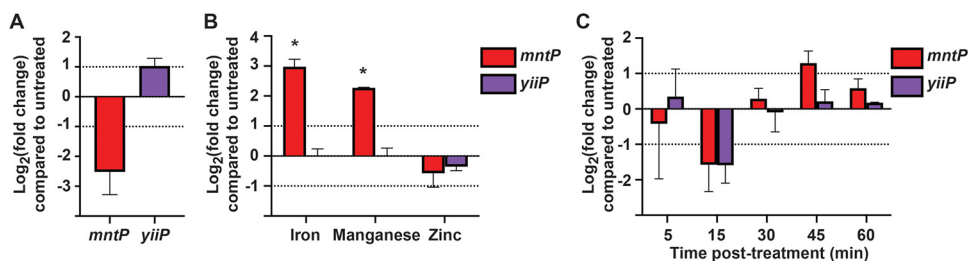
FIG 4 Expression of *mntP* increases in response to iron and manganese treatment, but *yiiP* does not. Log$_2$ fold change in expression for treated *S.* Typhimurium wild-type cultures, by comparison with untreated. Dotted lines represent the thresholds for significant expression change. (A) Expression of *mntP* and *yiiP* in LB supplemented with 3 mM EDTA. The apparent decrease in *mntP* expression failed to achieve statistical significance. (B) Expression of *mntP* in Tris minimal medium increased in response to 0.5 mM iron ($P = 0.014$) and 0.5 mM manganese ($P < 0.001$). (C) Expression of *mntP* and *yiiP* in LB with 2 mM DEANO. No statistically significant expression changes occurred. Data are the mean of 3 (A and B) or 4 (C) independent experiments. Error bars represent standard deviation. Statistical significance (*) was determined by a one-sample *t* test to a hypothetical mean of either 1 or −1.

YiiP contributes to manganese resistance in *S.* Typhimurium. Although expression of *yiiP* did not change in response to metal stress under our experimental conditions, the protein may be present due to constitutive expression and contribute to metal ion efflux. Building on the observations that YiiP shares homology with MntE (Fig. 3A) and its expression enhanced the zinc sensitivity of a zinc efflux mutant strain in a similar fashion to expression of MntP (Fig. 3B to D), a role in manganese efflux was investigated. To assess whether YiiP contributes to manganese resistance of *S.* Typhimurium, Δ*yiiP* and Δ*mntP* Δ*yiiP* strains were generated. The Δ*yiiP* strain grew similarly to the wild-type in the presence of 0.5 mM MnSO$_4$ (Fig. 5A). However, supplementation of the growth medium with 0.5 mM MnSO$_4$ delayed the growth of the Δ*mntP* strain and abrogated growth of the Δ*mntP* Δ*yiiP* strain (Fig. 5A). In spot assays, the Δ*mntP* Δ*yiiP* strain displayed decreased growth at 0.25 mM MnSO$_4$ and decreased survival at both 0.5 mM and 1 mM MnSO$_4$. By contrast, the Δ*mntP* strain only showed a moderate decrease in survival at 1 mM MnSO$_4$ (Fig. 5C). Taken together, these data show an enhancement of manganese sensitivity when both transporters are absent. Plasmid-based complementation with either *mntP* or *yiiP* expressed from the native promoter attenuated the growth defect of a Δ*mntP* Δ*yiiP* mutant, although the Δ*mntP* Δ*yiiP* p$_n$YiiP strain still had a minor growth delay relative to the wild-type and Δ*mntP* Δ*yiiP* p$_n$MntP strains (Fig. 5B). Similar complementation results were obtained in spot assays (Fig. 5D).

***S.* Typhimurium mutants lacking *mntP* and *yiiP* are neither sensitive to zinc nor disrupted for zinc homeostasis.** Previous experiments investigating the metal binding properties of recombinant *E. coli* YiiP revealed a capacity to interact with zinc ions *in vitro*, but not manganese (33, 38). Thus, the observed impact of manganese on the growth and survival of the *S.* Typhimurium Δ*mntP* Δ*yiiP* strain may reflect an indirect effect on zinc homeostasis. Interplay between zinc and manganese homeostasis has been shown to occur in several Gram-positive pathogens, such as *S. pneumoniae* where zinc has been established to disrupt manganese uptake and increase sensitivity to oxidative stress (39–42). However, this phenomenon has not been reported for the *Enterobacteriaceae* and, in *S.* Typhimurium, this may be attributable to the presence of the manganese-transporting natural resistance-associated macrophage protein (NRAMP) transporter MntH, which is not susceptible to zinc inhibition (9). By contrast, the impact of manganese on zinc homeostasis in *S.* Typhimurium has not been determined. Accordingly, we investigated whether the observed manganese sensitivity of the *S.* Typhimurium Δ*mntP* Δ*yiiP* strain was due to pleiotropic effects of perturbed zinc homeostasis.

Here, we examined the impact of zinc stress on the wild-type Δ*yiiP*, Δ*mntP*, and Δ*mntP* Δ*yiiP* strains. This revealed that zinc supplementation had no impact on the growth phenotype of any strain (Fig. 6A and B). These data indicate that *S.* Typhimurium zinc homeostasis is not dysregulated in the absence of manganese efflux. Furthermore, neither YiiP nor MntP contributes to substantially to zinc homeostasis. To further probe the impact on the zinc regulatory network of *S.* Typhimurium, the expression of genes controlled by the zinc uptake
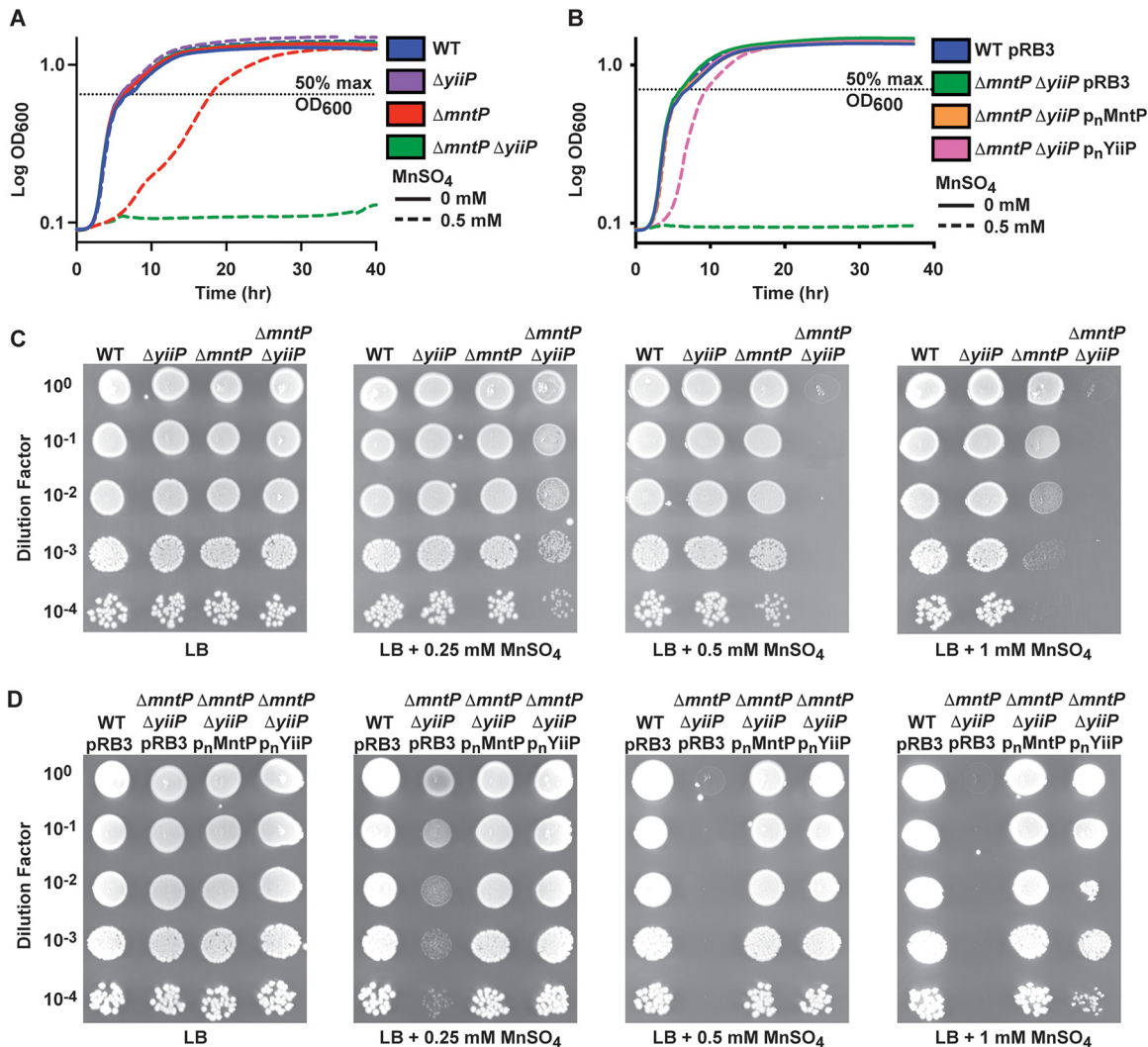
FIG 5 Manganese sensitivity of *S*. Typhimurium is enhanced in the absence of both *mntP* and *yiiP*. (A) Growth phenotypes of *S*. Typhimurium wild-type (WT), Δ*mntP*, Δ*yiiP*, and Δ*mntP* Δ*yiiP* strains in LB with or without 0.5 mM MnSO$_4$ supplementation. The Δ*mntP* strain was delayed exiting lag phase compared to WT in LB supplemented with 0.5 mM MnSO$_4$ ($P < 0.001$), and the Δ*mntP* Δ*yiiP* strain failed to grow. (B) Growth phenotypes of *S*. Typhimurium empty vector strains WT pRB3 and Δ*mntP* Δ*yiiP* pRB3 compared to plasmid-based complementation strains Δ*mntP* Δ*yiiP* p$_n$MntP and *mntP* Δ*yiiP* p$_n$YiiP in LB with or without 0.5 mM MnSO$_4$ supplementation. The expression constructs p$_n$MntP and p$_n$YiiP use the native promoters. Growth of *mntP* Δ*yiiP* p$_n$YiiP was delayed relative to WT ($P < 0.001$). Data for the growth curves (A) and (B) are the mean of 3 independent experiments. Statistical significance of the difference between the mutant strains and the wild-type was determined using the time (hr) to reach 50% maximum growth (OD$_{600}$; dashed line) and an unpaired two-tailed t test. (C) Growth of strains from (A) by spot plate assays. Dilutions of OD$_{600}$ = 0.3 cultures were spotted onto LB agar supplemented with MnSO$_4$ as shown. The Δ*mntP* Δ*yiiP* strain displayed decreased growth at 0.25 mM MnSO$_4$ and decreased survival at 0.5 mM and 1 mM. (D) Growth of strains from (B) by spot plate assays. Dilutions of OD$_{600}$ = 0.3 cultures were spotted onto LB agar supplemented with MnSO$_4$ as shown. A representative spot assay for each condition is shown, selected from 3 independent replicates. Expression of either YiiP or MntP complemented the survival defect of the Δ*mntP* Δ*yiiP* stain in the presence of MnSO$_4$.

regulator, Zur, and zinc export regulator, ZntR, were analyzed in the wild-type and Δ*mntP* Δ*yiiP* strains during exposure to excess manganese. The sensitivity of these metalloregulators is in the femtomolar to nanomolar range; thus, they provide a highly sensitive insight into cellular zinc homeostasis (43–45). Here, we monitored the expression of the Zur-regulated zinc uptake transporter *znuABC*, the primary *S*. Typhimurium pathway for zinc acquisition (46–48); the ZntR-regulated zinc exporter *zntA*, the major *S*. Typhimurium zinc efflux system (28, 49, 50); and *zupT*, which has been implicated in zinc and manganese import, although its regulatory control remains to be defined (14, 51, 52). These data show that there was no significant difference in expression of *zntA*, *znuC*, or *zupT* between the wild-type and Δ*mntP* Δ*yiiP* strains at 20 min (Fig. 6C) or 60 min (Fig. 6D) in the presence of
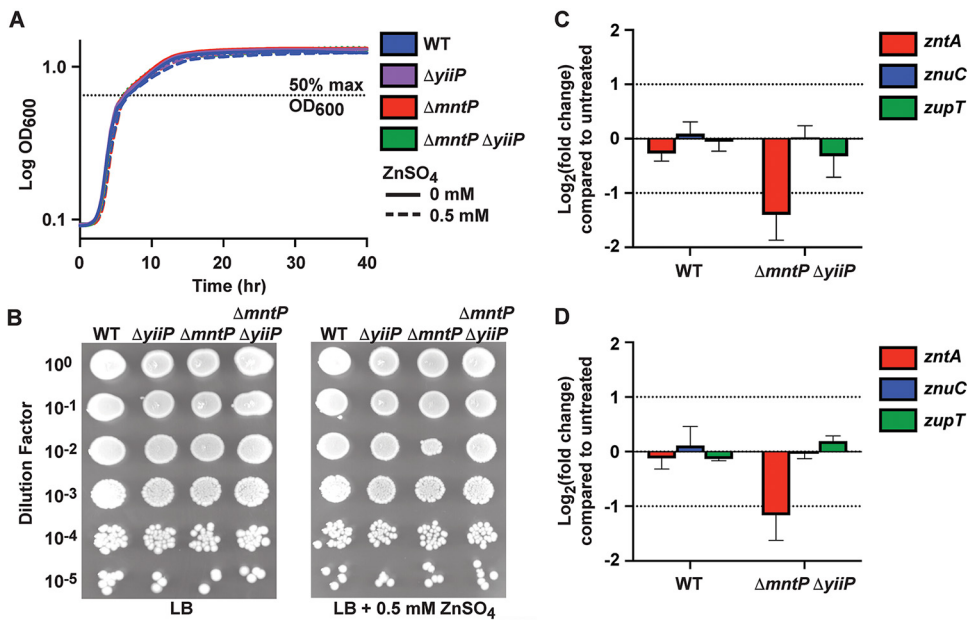
FIG 6 Zinc sensitivity is not enhanced in a Δ*mntP* Δ*yiiP* mutant, and expression of zinc-regulated transporters is not perturbed by manganese. (A) Growth of *S*. Typhimurium wild-type (WT) and the mutant derivatives Δ*yiiP*, Δ*mntP*, and Δ*mntP* Δ*yiiP* in LB with or without 0.5 mM ZnSO$_4$ supplementation. Data are the mean of 3 independent experiments, and statistical significance was determined by the time (hr) to reach 50% maximum growth (OD$_{600}$; dashed line) by unpaired two-tailed *t* test. (B) Growth of strains from (A) assessed using spot assays on LB agar supplemented with ZnSO$_4$ as shown. A representative spot assay for each condition is shown, selected from 3 independent replicates. (C) qPCR analyses of the zinc-regulated genes *zntA*, *znuC*, and *zupT* determined in response to challenge by 0.5 mM MnSO$_4$ (20 min exposure; OD$_{600}$ = 0.5 cultures). (D) qPCR analyses of the zinc-regulated genes *zntA*, *znuC*, and *zupT* determined in response to challenge by 0.5 mM MnSO$_4$ (60 min exposure; OD$_{600}$ = 0.5 cultures). Data in (C) and (D) are the mean (± standard deviation) of 3 independent experiments. Statistical significance was determined by a one-sample *t* test to a hypothetical mean of either 1 or −1. No significant differences were observed.

manganese. Thus, the *S*. Typhimurium Δ*mntP* Δ*yiiP* manganese-induced growth and survival defects (Fig. 5) are not an indirect effect arising from disrupted zinc homeostasis.

YiiP contributes to manganese efflux in *S*. Typhimurium. We next investigated whether YiiP participates in control of cellular manganese levels following exposure to NO·. It is important to note that in this experiment, direct comparisons are confined to the wild-type and the mutant strains within each analysis. This is due to differences in medium manganese concentrations that differed between the analyses (i.e., Fig. 7A vs. Fig. 7B), which influenced the absolute cellular abundances in the bacterial strains (43). Changes in cellular manganese followed generally similar patterns in the wild-type and Δ*yiiP* strains following treatment with 2 mM DEANO. However, manganese levels were elevated in the Δ*yiiP* strain relative to the wild-type strain at 5, 15, and 60 min (Fig. 7A). Manganese levels were greater in the Δ*mntP* Δ*yiiP* strain than in the wild-type at 5, 15, 45, and 60 min after treatment with 2 mM DEANO, but both strains reached a similar peak at 30 min (Fig. 7B). In the wild-type strain, cellular manganese decreased at 45 min compared to the 30 min peak and fell to pretreatment levels by 60 min. In the Δ*mntP* Δ*yiiP* strain, there was no significant difference in manganese levels at 30, 45, and 60 min posttreatment, suggesting that efflux was impaired when both genes were deleted (Fig. 7B).

Residue Asp45 is required for YiiP to alleviate manganese toxicity. Prior work has indicated that the A-site motif of CDF transporters dictates metal specificity (34, 35). For YiiP, the aspartate residue at position 45 has been implicated in facilitating transport of both cadmium and zinc in *in vitro* assays (35). When the aspartate residue was mutated to histidine (D45H), creating an HD-HD A-site motif in YiiP, the mutant protein transported zinc at similar rates as wild-type YiiP in *in vitro* assays, but no longer transported cadmium (35). In this study, our data indicate that *S*. Typhimurium YiiP is associated with physiological manganese export and do not support a role in zinc
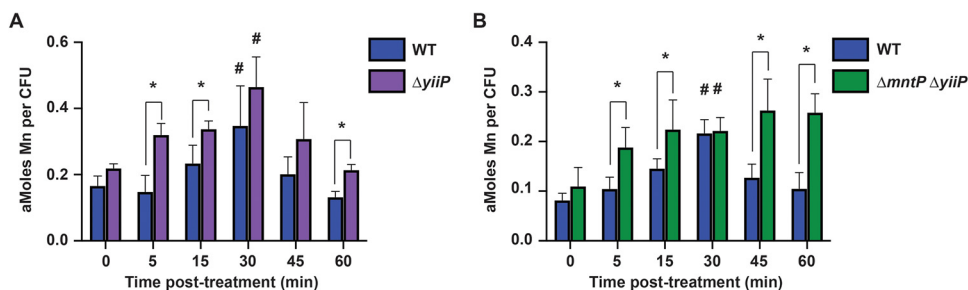
FIG 7 Intracellular manganese levels increase sooner in Δ*yiiP* and Δ*mntP* Δ*yiiP* mutants following NO· treatment and do not decrease in Δ*mntP* Δ*yiiP*. Total cellular manganese accumulation in wild-type (WT) and mutant *S.* Typhimurium cultures treated with 2 mM DEANO, determined by ICP-MS. (A) Intracellular manganese was greater in Δ*yiiP* *S.* Typhimurium than in WT (*) at 5 ($P = 0.004$), 15 ($P = 0.03$) and 60 min ($P = 0.001$) posttreatment. Manganese was elevated (#) in both WT ($P = 0.02$) and Δ*yiiP* ($P = 0.009$) at 30 min posttreatment compared to 0 min. (B) Intracellular manganese was greater in Δ*mntP* Δ*yiiP* *S.* Typhimurium than in WT (*) at 5 ($P = 0.01$), 15 ($P = 0.04$), 45 ($P = 0.008$), and 60 min ($P < 0.001$) posttreatment. Manganese was significantly elevated (#) in WT ($P < 0.001$) and Δ*mntP* Δ*yiiP* ($P = 0.003$) at 30 min posttreatment compared to 0 min. In WT, intracellular manganese was lower at 45 min than at 30 min ($P = 0.003$) and was no different than at 0 min by 60 min posttreatment. Intracellular manganese was no different in Δ*mntP* Δ*yiiP* at 45 and 60 min posttreatment than at 30 min. ICP-MS data are the mean of 4 independent experiments. Error bars represent standard deviation. Statistically significant differences across time points for each strain and between WT and mutant were determined by unpaired two-tailed *t* test.

homeostasis; however, this does not preclude a capacity for interaction with zinc *in vitro*. Here, we sought to determine the contribution of Asp45 to YiiP manganese transport. We generated a point mutation, substituting histidine for aspartate (D45H) in the p$_n$YiiP plasmid (p$_n$YiiP D45H). The mutant derivative was then investigated in a Δ*mntP* Δ*yiiP* background grown in medium supplemented with 0.5 mM MnSO$_4$. We observed that the growth phenotype of the Δ*mntP* Δ*yiiP* p$_n$YiiP D45H strain was no different than the Δ*mntP* Δ*yiiP* pRB3 strain (empty vector) in the presence of manganese, indicating a lack of complementation (Fig. 8A). To confirm that lack of complementation was due to lack of transporter function rather than protein instability, FLAG-tagged YiiP and YiiP D45H were expressed constitutively in the Δ*mntP* Δ*yiiP* background, subjected to SDS-PAGE and visualized by Western blot. Single bands of similar intensity were observed for both proteins at ~26 kDa (Fig. 8B). Although this is smaller than the predicted mass for YiiP (32.9 kDa), integral membrane proteins are known to show altered mass profiles in SDS-PAGE analyses. To confirm that the FLAG-tagged YiiP proteins were functional, spot assays were performed. Expression of YiiP:FLAG complemented the growth and survival defects of the Δ*mntP* Δ*yiiP* strain while expression of pYiiP D45H:FLAG did not (Fig. 8C). Collectively, these results show that Asp45 is required for manganese transport activity by *S.* Typhimurium YiiP.

DISCUSSION

Manganese efflux by MntP and the CDF transporter MntE has been studied in a variety of prokaryotic species, but thus far the presence of multiple manganese efflux systems within a single prokaryote has only been characterized in *B. subtilis*. *S.* Typhimurium encodes both an MntP homologue and YiiP, a CDF transporter. Identifying the target metal of CDF family transporters can be challenging despite efforts to establish the motifs that provide ion selectivity. YiiP has homology within the metal coordinating A-site to both zinc and manganese-transporting members of the CDF family (Fig. 3A) (36). YiiP from *E. coli* has been characterized as a zinc transporter using *in vitro* and structural methods, while an *in vivo* study linked its function to iron homeostasis. A physiological role for YiiP in zinc homeostasis has not yet been established in *S.* Typhimurium or *E. coli*, with Δ*yiiP* mutant strains not demonstrating zinc susceptible phenotypes (28, 29, 37). Here we show that expression of YiiP enhances the zinc sensitivity of Δ*zntA* Δ*zitB* *S.* Typhimurium rather than reducing it (Fig. 3B). These data, along with those showing enhanced manganese sensitivity and lack of manganese export in Δ*mntP* Δ*yiiP* *S.* Typhimurium (Fig. 5, 7B), suggest that zinc is not the cognate cargo of *S.* Typhimurium YiiP *in vivo*. Manganese transport phenotypes have been demonstrated *in vivo* for YiiP homologues
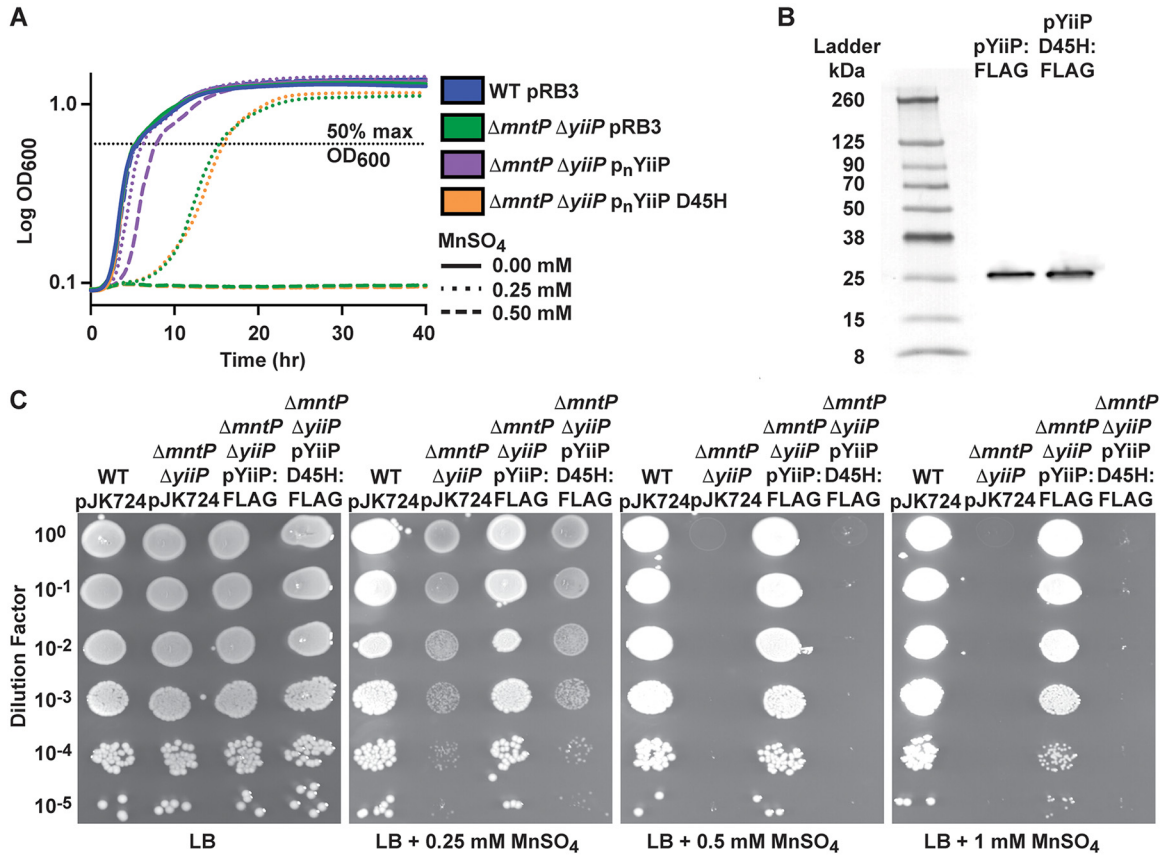
FIG 8 An aspartate residue at position 45 is required for manganese protection by YiiP. (A) Growth phenotypes of *S.* Typhimurium wild-type (WT pRB3), $\Delta mntP$ $\Delta yiiP$ pRB3, $\Delta mntP$ $\Delta yiiP$ p_nYiiP, and $\Delta mntP$ $\Delta yiiP$ p_nYiiP D45H strains in LB with or without MnSO$_4$ supplementation. The $\Delta mntP$ $\Delta yiiP$ pRB3 and $\Delta mntP$ $\Delta yiiP$ p_nYiiP D45H strains failed to grow in 0.5 mM MnSO$_4$. In 0.25 mM MnSO$_4$ there was no difference between $\Delta mntP$ $\Delta yiiP$ pRB3 and $\Delta mntP$ $\Delta yiiP$ p_nYiiP D45H. Both strains were delayed for growth in 0.25 mM MnSO$_4$ compared to WT pRB3 ($P < 0.001$) and $\Delta mntP$ $\Delta yiiP$ p_nYiiP ($P < 0.001$). Data are the mean of 3 independent experiments, and statistical significance was determined by the time (hr) to reach 50% maximum growth (OD$_{600}$; dashed line) by unpaired two-tailed *t* test. (B) Western blot of FLAG-tagged YiiP and YiiP D45H expressed in *S.* Typhimurium $\Delta mntP$ $\Delta yiiP$ shown adjacent to a visible protein standard. Single bands of equal intensity were observed for both versions of the YiiP protein at an apparent size of ∼26 kDa. (C) Spot plate assays of *S.* Typhimurium WT, $\Delta mntP$ $\Delta yiiP$, and the $\Delta mntP$ $\Delta yiiP$ complemented strains encoding FLAG-tagged fusion variants of YiiP and YiiP D45H on LB with and without MnSO$_4$ supplementation. A representative spot assay for each condition is shown, selected from 3 independent replicates. The $\Delta mntP$ $\Delta yiiP$ strain expressing YiiP D45H:FLAG displays the same phenotype as the $\Delta mntP$ $\Delta yiiP$ empty vector strain.

from *Sinorhizobium meliloti*, *Deinococcus radiodurans*, and *Rhizobium etli* (53–55). These proteins share a clade with YiiP from *E. coli* that is phylogenetically distinct from the clades containing the well-characterized CDF zinc transporters CzcD and ZitB (54, 56). The variety of proposed substrates for transporters within this clade is diverse while relatively few transporters have been experimentally characterized. Further work will be required to gain an accurate understanding of the biological functions of this group of transporters.

While function of MntP alone was sufficient to provide protection from manganese toxicity under the conditions of this study, deletion of both *mntP* and *yiiP* enhanced the sensitivity of *S.* Typhimurium to manganese intoxication (Fig. 5A and C). Function of either MntP or YiiP could restore manganese homeostasis following NO· treatment, and only the $\Delta mntP$ $\Delta yiiP$ strain was abrogated for manganese efflux during the late-stage response to NO· exposure (Fig. 7B). Selectivity for manganese depends on residue Asp45 within the A-site metal binding region of YiiP. A change in transport activity in response to mutation of Asp45 is consistent with similar results arising from the mutation of A-sites in *E. coli* YiiP and other CDF transporters (34, 35). While we cannot exclude the possibility that YiiP might facilitate the transport of other transition metal cations under certain conditions, the results of this study support a role for YiiP as a manganese exporter in *S.* Typhimurium.

Regulation of *yiiP* expression remains an open question. Unlike *mntP*, it is not part of the MntR regulon and has not been shown to be part of the Fur, Zur, or ZntR regulons (26, 57). Expression of *mntP* is regulated by both MntR and the *ybbP-ykoY* manganese-sensing riboswitch in *E. coli* (58). The promoter region of *mntP* from *S.* Typhimurium shows homology to that of *E. coli*, suggesting that similar regulatory mechanisms may apply to *mntP* expression in both organisms. By contrast, the promoter region of *yiiP* lacks this homology. Induction of *mntP* expression occurred in response to manganese and iron stress, whereas *yiiP* expression was unaffected by the conditions tested (Fig. 4B). Previous work using β-galactosidase fusions to the *yiiP* promoter in *E. coli* showed upregulation in response to zinc and a modest response to iron after several hours of incubation (29, 30). Since none of the known metal-responsive regulators have been implicated in *yiiP* expression, any expression change in response to metal excess may be indirect and more time may be necessary for the cellular conditions driving regulation to develop. Alternatively, expression of *yiiP* may be constitutive in *S.* Typhimurium under standard laboratory growth conditions. Constitutive expression would be consistent with the more rapid accumulation of manganese observed in strains lacking *yiiP* (Fig. 7), while a strain lacking only the inducible *mntP* acquires manganese similarly to the wild-type (Fig. 2). Expression of *mntE*, the CDF manganese transporter from *S. pneumoniae*, does not respond to manganese abundance and has been proposed to be expressed constitutively (19). Manganese efflux activity in *E. coli* is further regulated by the small protein MntS. *E. coli* that overexpress MntS display enhanced manganese accumulation and have the same manganese-sensitive phenotype as Δ*mntP* mutants, suggesting that this small protein may function to prevent the efflux activity of MntP (16). Overexpression of MntS in a Δ*mntP* strain did not enhance the manganese sensitivity of this mutant, suggesting that it does not inhibit the function of additional manganese exporters such as YiiP, but this possibility has not yet been investigated directly.

While efflux by either MntP or YiiP is sufficient to restore baseline manganese levels in *S.* Typhimurium following NO· exposure, and both contribute to protecting *S.* Typhimurium from excess manganese in culture, the broader functional significance of these transporters in *S.* Typhimurium biology and pathogenesis has yet to be determined. Manganese acquisition is required for *S.* Typhimurium infection and virulence, but what role, if any, efflux might play is not currently known (10, 11). Manganese efflux has been shown to play an important role in the virulence of other pathogens such as *S. pneumoniae* and *S. aureus* and in colonization by *E. faecalis* (19–21). Although manganese has primarily been understood to act as an antioxidant, and absence of *mntE* rendered *S. pneumoniae* more resistant to both NO· and oxidative stress in the form of methyl viologen, this has not been the case for all organisms and oxidants (19). *S. aureus* lacking *mntE* was more sensitive to sodium hypochlorite (NaOCl), while *S. pyogenes* was more sensitive to peroxide (H_2O_2) (20, 22). Manganese excess has been shown to affect electron transport chain function and function of Fe-S cluster enzymes in central energy-generating pathways. (15–17). These proteins are also targets of oxidants, which could explain, at least in part, why enhanced sensitivity to oxidants is seen for some species, but the mechanisms underlying the requirement for manganese efflux remain incompletely understood. In light of these data, the dynamic flux of multiple metals that occurs in response to NO·, and the varied environments and stresses encountered by pathogens within the host, characterizing the biological roles of microbial manganese efflux systems, is an open and potentially complex area of investigation. Based on the findings of this study, we suggest that any future work concerning the biological significance of manganese efflux in *S.* Typhimurium should address both the function of MntP and the newly established manganese export function of YiiP.

MATERIALS AND METHODS

Bioinformatic analysis. *S.* Typhimurium homology matches to MntP from *Escherichia coli* MG1655 and MntE and CzcD from *Streptococcus pneumoniae* TIGR4 were determined using BLASTP from the Kyoto Encyclopedia of Genes and Genomes (KEGG) website with default settings. Alignments were generated using the KEGG ClustalW tool (59). Alignment graphics were generated using BoxShade hosted by ExPASy, the Swiss Institute of Bioinformatics Resource Portal (https://embnet.vital-it.ch/software/BOX_form.html).

Growth conditions. *Salmonella enterica* serovar Typhimurium and *Escherichia coli* were grown in Luria-Bertani medium (LB; Fisher) at 37°C with shaking at 250 rpm unless otherwise specified. Antibiotic selection

TABLE 1 Strains and plasmids

Plasmid or strain	Genotype	Source
pKD46	*bla araC*-P$_{araB}$-γβ *exo* oriR101 repA101ts	(60)
pKD3	*bla FRTcatFRT* PS1 PS2 oriRγ	(60)
pKD4	*bla FRTaphFRT* PS1 PS2 oriRγ	(60)
pCP20	*bla cat* cI857 IPr *flp* PSC101 oriTS	(60)
pRB3-273C (pRB3)	*bla par* RK2 oriV *trfA*	(62)
pJK724	*bla par* RK2 oriV *tfrA* P$_{trc}$	(63)
pEF101 (p$_n$MntP)	bla par RK2 oriV tfrA P$_{native}$-mntP	This study
pEF102 (p$_n$YiiP)	bla par RK2 oriV tfrA P$_{native}$-yiiP	This study
pEF103 (pYiiP)	bla par RK2 oriV tfrA P$_{trc}$-yiiP	This study
pEF106 (pMntP)	*bla par* RK2 oriV *tfrA* P$_{trc}$-mntP	This study
pEF108 (p$_n$YiiP D45H)	bla par RK2 oriV tfrA P$_{native}$-yiiP D45H	This study
pEF115 (pYiiP:FLAG)	bla par RK2 oriV tfrA P$_{trc}$-yiiP:FLAG	This study
pEF116 (pYiiP D45H:FLAG)	bla par RK2 oriV tfrA P$_{trc}$-yiiP D45H:FLAG	This study
JK237 (WT)	14028s	ATCC
JK895(FLS187)	14028s/pRB3-273C	(65)
EF560	Δ*yiiP::frt-kan-frt*	This study
EF561	Δ*yiiP::frt-cm-frt*	(28)
EF564	14028s/pJK724	(14)
EF610	Δ*fljBA::FRT fliC5569::tetRA* (+1UTR)	(14)
EF635	Δ*mntP::frt-cm-frt*	This study
EF657	Δ*mntP::frt-cm-frt* Δ*yiiP::frt-kan-frt*	This study
EF697	Δ*fljBA::FRT fliC5569::tetRA* (+1UTR) Δ*mntP::frt-cm-frt*	This study
EF698	Δ*fljBA::FRT fliC5569::tetRA* (+1UTR) Δ*yiiP::frt-kan-frt*	This study
EF701	Δ*fljBA::FRT fliC5569::tetRA* (+1UTR) Δ*mntP::frt-cm-frt* Δ*yiiP::frt-kan-frt*	This study
EF725	Δ*mntP::FRT* Δ*yiiP::FRT*	This study
EF737	Δ*mntP::frt-cm-frt*/pRB3-273C	This study
EF738	Δ*mntP::frt-cm-frt*/pEF101	This study
EF739	Δ*mntP::frt-cm-frt* Δ*yiiP::frt-kan-frt*/pRB3-273C	This study
EF740	Δ*mntP::frt-cm-frt* Δ*yiiP::frt-kan-frt*/pEF101	This study
EF741	Δ*mntP::frt-cm-frt* Δ*yiiP::frt-kan-frt*/pEF102	This study
EF745	Δ*zntA::frt-cm-frt* Δ*zitB::frt-kan-frt*/ pJK724	This study
EF746	Δ*zntA::frt-cm-frt* Δ*zitB::frt-kan-frt*/ pEF103	This study
EF747	Δ*mntP::frt-cm-frt* Δ*yiiP::frt-kan-frt*/pJK724	This study
EF754	Δ*yiiP::frt-kan-frt*	This study
EF755	Δ*mntP::FRT*	This study
EF762	Δ*zntA::frt-cm-frt* Δ*zitB::frt-kan-frt*/ pEF106	This study
EF773	Δ*mntP::frt-cm-frt* Δ*yiiP::frt-kan-frt*/pEF108	This study
EF829	Δ*mntP::frt-cm-frt* Δ*yiiP::frt-kan-frt*/pEF115	This study
EF830	Δ*mntP::frt-cm-frt* Δ*yiiP::frt-kan-frt*/pEF116	This study

was used for strain construction only at the following concentrations: 100 μg mL^{-1} ampicillin (Amp), 50 μg mL^{-1} kanamycin (Kan), and 20 μg mL^{-1} chloramphenicol (Cm).

Strain and plasmid construction. All strains and plasmids are listed in Table 1. All primers are listed in Table 2. *S.* Typhimurium strains were generated in the ATCC 14028s genetic background, which also served as the wild-type strain in this study (JK237). Deletion mutants were constructed using λ-RED mediated recombination with either pKD3 or pKD4 as the template (60). Expression of Flp-FRT recombinase from pCP20 was used to remove the antibiotic resistance cassettes from strains EF657 and EF635 to generate strains EF725 and EF755 (60). Combination mutants were created using P22HT105/int bacteriophage transduction (61). All mutants were verified by PCR.

E. coli strain TB1 was used as the cloning host strain. Purified genomic DNA from *S.* Typhimurium 14028s was used as the PCR template unless otherwise specified. Plasmids pEF101 and pEF102 were generated by amplifying the upstream promoter region and coding sequence of *mntP* using primers EFP334 and EFP335 and *yiiP* using primers EFP336 and EFP340. Amplified fragments were digested with

TABLE 2 Primer sequences

Primer	Sequence 5′–3′	Purpose
EFP21	CGACATCATAACGGTTCTGGC	Sequencing of pEF103, pEF106
EFP300	ATGTTTGCTGGGGGGCAGTGATGTGTTTAATGGATACCCCGGTGTAGGCTGGAGCTGCTTC	Creation of EF635
EFP301	TTAACCGTGAAAATGCGTCCAGAGGATCTGGACGCCAATTCATATGAATATCCTCCTTAG	Creation of EF635
EFP306	ATGTTAATGTTGCGCCGTCAATTGG	EF635 validation
EFP319	CACCCATGGCCATGAATCAAACCTATGGACGGC	Creation of pEF103
EFP320	CACAAGCTTTTATACAAGCTCGAACTTCCTGCC	Creation of pEF103
EFP334	GCGGGTACCAACTTCTTATTGAAAATCAATATC	Creation of pEF101
EFP335	ATAAAGCTTTTAACCGTGAAAATGCGTCCAG	Creation of pEF101, pEF106
EFP336	ATAGGTACCCCCTGTTTTCCTTGCCATAGACACC	Creation of pEF102
EFP340	GCGAAGCTTTTATACAAGCTCGAACTTCCTGCC	Creation of pEF102
EFP346	AAACCATGGCAATGTTTGCTGGGGGCAGTG	Creation of pEF106
EFP347	AATATCCACCAGCGAGTGCACCAACGC	Creation of pEF108
EFP397	CACAAGCTTTTACTTGTCGTCATCGTCTTTGTAGTCTAGCTCAACGAACTTCCTGCC	Creation of pEF115, pEF116
JKP227	ACTCATTAGGCACCCCAGGC	Sequencing of pEF101, pEF102
JKP244	CTCTTCGCTATTACGCCAGC	Sequencing of pEF101, pEF102
JKP744	CCTATGGACGGCTGGTTAGCCGGGCGGCTATCGCGGCAACGTGTAGGCTGGAGCTGCTTC	Creation of EF560, EF561
JKP745	AATGACATCTGAACCCGGAAAACGCTGTAAAATCGCCTGCCATATGAATATCTCCTTAG	Creation of EF560, EF561
JKP746	TGAAAAGCATCAGCAACGAA	EF560, EF561 validation
JKP747	CCGATTTTCTTAATCATGACTACC	EF560, EF561 validation
JKP777	CACTTCTGAGTTCGGCATGG	Sequencing of pEF103, pEF106
rpoD qPCR fwd	GTGAAATGGGCACTGTTGAAC	*rpoD* qPCR
rpoD qPCR rev	TTCCAGCAGATAGGTAATGGC	*rpoD* qPCR
yiiP qPCR fwd	ACTCGCTGGTGGATATTGCC	*yiiP* qPCR
yiiP qPCR rev	ACAGAAACAACGCCGAACCG	*yiiP* qPCR
mntP qPCR fwd	GCGTACCGGTCTTATCTTTGG	*mntP* qPCR
mntP qPCR rev	GCTATCCAGTGGTTCCATTCC	*mntP* qPCR
zntA qPCR fwd	TCTGTATCCTATTGCCCGCC	*zntA* qPCR
zntA qPCR rev	CAATAAACAGCGCGCCAATG	*zntA* qPCR
znuC qPCR fwd	GGGGAAGTCAACGCTTGTAC	*znuC* qPCR
znuC qPCR rev	TTTGCGGGACATAGCCGATA	*znuC* qPCR
zupT qPCR fwd	GATCATGCTGCTTATCTCGCTG	*zupT* qPCR
zupT qPCR rev	CCAGATCCTGCGGATGAGCGTG	*zupT* qPCR

KpnI and HindIII then ligated into pRB3-273C digested with the same enzymes in reverse orientation to the multiple cloning site promoter (62). Constructs were confirmed by sequencing with JKP227 and JKP244 then transformed into strain EF657 to generate strains EF744 and EF745. To generate plasmids pEF103 and pEF106, the coding sequence of *yiiP* was amplified using primers EFP319 and EFP320 and the coding sequence of *mntP* was amplified using primers EFP346 and EFP335. Amplified fragments were digested with NcoI and HindIII then ligated into pJK724 digested with the same enzymes (63). Constructs were sequenced using primers EFP21 and JKP777 then transformed into zinc efflux mutant strain EF528 to generate strains EF746 and EF762. To generate plasmid pEF108, primers EFP336 and EFP347 were used to amplify a short fragment containing the target mutation (D45H). The fragment was purified from an agarose gel then used in a second amplification reaction with EFP340. Full-length product was digested with KpnI and HindIII then ligated into pRB3-273C digested with the same enzymes in reverse orientation to the multiple cloning site promoter. The construct was verified by sequencing with JKP227 and JKP244 then transformed into strain EF657 to generate strain EF773. Plasmids pEF115 and pEF116 were generated by amplifying the coding sequences of plasmids pEF102 and pEF108 using primers EFP319 and EFP397. Amplified fragments were digested with NcoI and HindIII then ligated into pJK724 digested with the same enzymes. Constructs were sequenced using primers EFP21 and JKP777 then transformed into strain EF657 to generate strains EF829 and EF830.

Metal sensitivity growth curve assays. To determine manganese sensitivity, wild-type *S.* Typhimurium (JK237) and transporter mutants (EF561, EF635, EF657) were grown overnight in LB, normalized to optical density at 600 nm (OD_{600}) of 1, and diluted in triplicate 1:1000 into LB or LB with 0.5 mM $MnSO_4$ for a final volume of 300 μL in a flat-bottom 96-well nontreated tissue culture microtiter plate (Midwest Scientific). Cultures were grown aerobically with shaking at 567 rpm (3 mm) in a Biotek Synergy HTX multimode 96-well plate reader at 37°C. Growth was monitored by recording OD_{600} every 15 min for 40 h. Statistical significance was determined by comparing the time required to reach 50% maximum OD_{600} by unpaired two-tailed *t* test using Microsoft Excel.

Complementation of Δ*mntP* was assessed using strains JK895, EF737, and EF738. Complementation of Δ*mntP* Δ*yiiP* was assessed using JK895, EF739, EF740, and EF741. Complementation of Δ*mntP* Δ*yiiP* with the YiiP D45H mutant construct pEF108 was assessed using strains JK895, EF739, EF741, and EF773. Growth assays were carried out as described above except $MnSO_4$ was added at both 0.5 mM and 0.25 mM final concentration.

Strains used to determine zinc sensitivity in response to YiiP and MntP expression were EF564, EF745, EF746, and EF762. Zinc sensitivity of manganese transporter mutants was assessed using strains JK237, EF561, EF635, and EF657. Zinc sensitivity assays were carried out as described above but the LB was supplemented with 0.125 mM or 0.5 mM $ZnSO_4$ respectively.

Metal sensitivity spot assays. Strains were grown overnight in LB, diluted 1:1000 in 5 mL fresh medium then grown with shaking at 37°C for 3 h to OD_{600} = 0.3. Cultures were serially diluted 10-fold in PBS, then 3 μL were spotted onto LB agar plates with or without metal sulfate supplementation. Plates were grown 14–16 h at 37°C prior to imaging. Spot assays utilized the same strains as growth curve assays. Complementation of manganese sensitivity by expression of FLAG-tagged YiiP proteins was assessed using strains EF564, EF747, EF829, and EF830.

Metal content analyses. Inductively coupled plasma-mass spectrometry (ICP-MS) analyses were conducted using strain variants that were also flagellar mutants (EF610, EF697, EF698, EF701) to increase pelleting efficiency as in previous studies (14, 28). Overnight cultures were diluted 1:1000 into 100 mL fresh LB medium and then grown to OD_{600} ~ 1. Cultures were divided into 5 mL aliquots in 18 × 150 mm glass tubes, treated with 2 mM diethylamine NONOate (DEANO) and returned to shaking at 37°C. At 0, 5, 15, 30, 45, and 60 min posttreatment, 4.5 ml of culture was pelleted by centrifugation then washed twice with ultrapure water. Pellets were resuspended in analytical grade nitric acid, boiled, then diluted 1:10 with ultrapure water for analysis on an Agilent 8900x QQQ ICP-MS. Bacterial numbers, defined as CFU, were enumerated at each time point for calculation of relative metal concentrations. Statistical significance was determined by two-tailed *t* test in Microsoft Excel.

Gene expression analysis. Primer sequences used for expression analysis are listed in Table 2. For expression under metal chelation, wild-type *S.* Typhimurium was grown overnight, diluted 1:1000 in 2 × 5 mL fresh LB medium, and grown to OD_{600} ~ 1. Ethylenediaminetetraacetic acid (EDTA) at a concentration of 3 mM was added to one of the cultures for 20 min. 1.5 ml of each culture was pelleted by centrifugation then resuspended in 800 μL TRIzol for RNA isolation.

For analysis of expression in response to metal supplementation, overnight LB cultures were diluted 1:1000 into 25 mL modified Tris minimal medium (50 mM Tris, 80 mM NaCl, 2 mM KCl, 5 mM NH_4SO_4, 1.65 mM $Na_2SO_4 \cdot 10H_2O$, 1 mM $MgSO_4 \cdot 6H_2O$, 0.3 mM $CaCl_2$, 1.6 mM Na_2HPO_4, 0.2% glucose, 3 g.L^{-1} casamino acids) and grown to OD_{600} ~ 0.5. The culture was subdivided into 4 × 5 mL cultures in 18 × 150 mm glass tubes. One was left untreated and the others were supplemented with 0.5 mM $FeSO_4$ plus 1 mM ascorbate, 0.5 mM $MnSO_4$, or 0.5 mM $ZnSO_4$. After 20 min, 3 mL of culture was pelleted by centrifugation and pellets were resuspended in 800 μL TRIzol for RNA isolation.

To monitor expression in response to nitrosative stress, wild-type *S.* Typhimurium was grown overnight, diluted 1:1000 in 100 mL fresh LB medium, and grown to OD_{600} ~ 1. The culture was subdivided into 5 duplicate pairs of 5 mL cultures in 18 × 150 mm glass tubes. One set was treated with 2 mM DEANO and one set left untreated. Cultures were returned to shaking at 37°C. At 5, 15, 30, 45, and 60 min posttreatment, 1.5 ml of treated and untreated culture was pelleted by centrifugation then resuspended in 800 μL TRIzol for RNA isolation.

To determine whether supplementation of growth medium with manganese disrupts zinc homeostasis and expression of zinc-regulated zinc transporters, JK237 and EF657 *S.* Typhimurium were grown overnight, diluted 1:1000 in 2 × 5 mL fresh LB medium, and grown to OD_{600} ~ 0.5. One culture was left untreated and the other was supplemented with 0.5 mM $MnSO_4$ before cultures were returned to shaking at 37°C. At 20 and 60 min posttreatment, 1.5 mL of treated and untreated culture was pelleted by centrifugation then resuspended in 800 μL TRIzol for RNA isolation.

For all analyses, RNA and cDNA were prepared as described previously (64). Quantitative PCR (qPCR) was carried out using SYBR green on a Bio-Rad CFX96 real-time system with *rpoD* as the internal control for normalization. Fold change values (treated/untreated) were log_2 transformed prior to plotting. Statistical significance was determined by one-sample *t* test compared to a hypothetical means of 1 or −1 using GraphPad Prism.

Western blotting. Strains EF829 and EF830 were grown as for spot assays, then 3 mL of culture was pelleted, resuspended in 100 μL PBS, and diluted 1:1 in 2× Laemmli sample buffer (Bio-Rad) with DTT (100 mM final). Samples were incubated 60 min at 55°C before 7.5 μL was loaded on a 4–20% Tris-glycine gel for separation in Tris-glycine-SDS buffer (Bio-Rad). Separated proteins were transferred to nitrocellulose membranes, which were blocked with EveryBlot Blocking Buffer (Bio-Rad) then probed with 1:000 monoclonal anti-FLAG M2-peroxidase (HRP) antibody (Millipore Sigma). Blots were visualized using an ECL Western blotting analysis system (Amersham) on an ImageQuant LAS 4000 imaging system (GE Healthcare) that captures both chemiluminescent and visible images. The visible image of the protein size standards was aligned with the chemiluminescent image of the same blot.

REFERENCES

1. Andreini C, Bertini I, Cavallaro G, Holliday GL, Thornton JM. 2008. Metal ions in biological catalysis: from enzyme databases to general principles. J Biol Inorg Chem 13:1205–1218. https://doi.org/10.1007/s00775-008-0404-5.

2. Waldron KJ, Rutherford JC, Ford D, Robinson NJ. 2009. Metalloproteins and metal sensing. Nature 460:823–830. https://doi.org/10.1038/nature08300.

3. Hmiel SP, Snavely MD, Florer JB, Maguire ME, Miller CG. 1989. Magnesium transport in *Salmonella* Typhimurium: genetic characterization and cloning of three magnesium transport loci. J Bacteriol 171:4742–4751. https://doi.org/10.1128/jb.171.9.4742-4751.1989.

4. Snavely MD, Florer JB, Miller CG, Maguire ME. 1989. Magnesium transport in *Salmonella* Typhimurium: $28Mg^{2+}$ transport by the CorA, MgtA, and MgtB systems. J Bacteriol 171:4761–4766. https://doi.org/10.1128/jb.171.9.4761-4766.1989.

5. Cartron ML, Maddocks S, Gillingham P, Craven CJ, Andrews SC. 2006. Feo–transport of ferrous iron into bacteria. Biometals 19:143–157. https://doi.org/10.1007/s10534-006-0003-2.

6. Crouch M-LV, Castor M, Karlinsey JE, Kalhorn T, Fang FC. 2008. Biosynthesis and IroC-dependent export of the siderophore salmochelin are essential for virulence of *Salmonella enterica* serovar Typhimurium. Mol Microbiol 67:971–983. https://doi.org/10.1111/j.1365-2958.2007.06089.x.

7. Ammendola S, Pasquali P, Pistoia C, Petrucci P, Petrarca P, Rotilio G, Battistoni A. 2007. High-affinity Zn^{2+} uptake system ZnuABC is required for bacterial zinc homeostasis in intracellular environments and contributes to the virulence of *Salmonella enterica*. Infect Immun 75:5867–5876. https://doi.org/10.1128/IAI.00559-07.

8. Kehres DG, Zaharik ML, Finlay BB, Maguire ME. 2000. The NRAMP proteins of *Salmonella* Typhimurium and *Escherichia coli* are selective manganese transporters involved in the response to reactive oxygen. Mol Microbiol 36:1085–1100. https://doi.org/10.1046/j.1365-2958.2000.01922.x.

9. Kehres DG, Janakiraman A, Slauch JM, Maguire ME. 2002. SitABCD Is the alkaline Mn^{2+} transporter of *Salmonella enterica* serovar Typhimurium. J Bacteriol 184:3159–3166. https://doi.org/10.1128/JB.184.12.3159-3166.2002.

10. Boyer E, Bergevin I, Malo D, Gros P, Cellier MFM. 2002. Acquisition of Mn(II) in addition to Fe(II) is required for full virulence of *Salmonella enterica* serovar Typhimurium. Infect Immun 70:6032–6042. https://doi.org/10.1128/IAI.70.11.6032-6042.2002.

11. Diaz-Ochoa VE, Lam D, Lee CS, Klaus S, Behnsen J, Liu JZ, Chim N, Nuccio S-P, Rathi SG, Mastroianni JR, Edwards RA, Jacobo CM, Cerasi M, Battistoni A, Ouellette AJ, Goulding CW, Chazin WJ, Skaar EP, Raffatellu M. 2016. *Salmonella* mitigates oxidative stress and thrives in the inflamed gut by evading calprotectin-mediated manganese sequestration. Cell Host Microbe 19:814–825. https://doi.org/10.1016/j.chom.2016.05.005.

12. Imlay JA. 2014. The mismetallation of enzymes during oxidative stress. J Biol Chem 289:28121–28128. https://doi.org/10.1074/jbc.R114.588814.

13. Kehres DG, Maguire ME. 2003. Emerging themes in manganese transport, biochemistry and pathogenesis in bacteria. FEMS Microbiol Rev 27:263–290. https://doi.org/10.1016/S0168-6445(03)00052-4.

14. Yousuf S, Karlinsey JE, Neville SL, McDevitt CA, Libby SJ, Fang FC, Frawley ER. 2020. Manganese import protects *Salmonella enterica* serovar Typhimurium against nitrosative stress. Metallomics 12:1791–1801. https://doi.org/10.1039/d0mt00178c.

15. Kaur G, Kumar V, Arora A, Tomar A, Ashish Sur R, Dutta D. 2017. Affected energy metabolism under manganese stress governs cellular toxicity. Sci Rep 7:11645. https://doi.org/10.1038/s41598-017-12004-3.

16. Martin JE, Waters LS, Storz G, Imlay JA. 2015. The *Escherichia coli* small protein MntS and exporter MntP optimize the intracellular concentration of manganese. PLoS Genet 11:e1004977. https://doi.org/10.1371/journal.pgen.1004977.

17. Sachla AJ, Luo Y, Helmann JD. 2021. Manganese impairs the QoxABCD terminal oxidase leading to respiration-associated toxicity. Mol Microbiol 116:729–742. https://doi.org/10.1111/mmi.14767.

18. Kolaj-Robin O, Russell D, Hayes KA, Pembroke JT, Soulimane T. 2015. Cation Diffusion Facilitator family: structure and function. FEBS Lett 589:1283–1295. https://doi.org/10.1016/j.febslet.2015.04.007.

19. Rosch JW, Gao G, Ridout G, Wang Y-D, Tuomanen EI. 2009. Role of the manganese efflux system *mntE* for signalling and pathogenesis in *Streptococcus pneumoniae*. Mol Microbiol 72:12–25. https://doi.org/10.1111/j.1365-2958.2009.06638.x.

20. Grunenwald CM, Choby JE, Juttukonda LJ, Beavers WN, Weiss A, Torres VJ, Skaar EP. 2019. Manganese detoxification by MntE is critical for resistance to oxidative stress and virulence of *Staphylococcus aureus*. mBio 10:e02915-18. https://doi.org/10.1128/mBio.02915-18.

21. Lam LN, Wong JJ, Chong KKL, Kline KA. 2020. *Enterococcus faecalis* manganese exporter MntE alleviates manganese toxicity and is required for mouse gastrointestinal colonization. Infect Immun 88. https://doi.org/10.1128/IAI.00058-20.

22. Turner AG, Ong C-LY, Gillen CM, Davies MR, West NP, McEwan AG, Walker MJ. 2015. Manganese homeostasis in group A *Streptococcus* is critical for resistance to oxidative stress and virulence. mBio 6:e00278-15. https://doi.org/10.1128/mBio.00278-15.

23. Huang X, Shin J-H, Pinochet-Barros A, Su TT, Helmann JD. 2017. *Bacillus subtilis* MntR coordinates the transcriptional regulation of manganese uptake and efflux systems. Mol Microbiol 103:253–268. https://doi.org/10.1111/mmi.13554.

24. Padilla-Benavides T, Long JE, Raimunda D, Sassetti CM, Argüello JM. 2013. A novel P(1B)-type Mn^{2+}-transporting ATPase is required for secreted protein metallation in mycobacteria. J Biol Chem 288:11334–11347. https://doi.org/10.1074/jbc.M112.448175.

25. Li C, Tao J, Mao D, He C. 2011. A novel manganese efflux system, YebN, is required for virulence by *Xanthomonas oryzae* pv. *oryzae*. PLoS One 6:e21983. https://doi.org/10.1371/journal.pone.0021983.

26. Waters LS, Sandoval M, Storz G. 2011. The *Escherichia coli* MntR miniregulon includes genes encoding a small protein and an efflux pump required for manganese homeostasis. J Bacteriol 193:5887–5897. https://doi.org/10.1128/JB.05872-11.

27. Veyrier FJ, Boneca IG, Cellier MF, Taha M-K. 2011. A novel metal transporter mediating manganese export (MntX) regulates the Mn to Fe intracellular ratio and *Neisseria meningitidis* virulence. PLoS Pathog 7:e1002261. https://doi.org/10.1371/journal.ppat.1002261.

28. Frawley ER, Karlinsey JE, Singhal A, Libby SJ, Doulias P-T, Ischiropoulos H, Fang FC. 2018. Nitric oxide disrupts zinc homeostasis in *Salmonella enterica* serovar Typhimurium. mBio 9:e01040-18.

29. Grass G, Fan B, Rosen BP, Franke S, Nies DH, Rensing C. 2001. ZitB (YbgR), a member of the cation diffusion facilitator family, is an additional zinc transporter in *Escherichia coli*. J Bacteriol 183:4664–4667. https://doi.org/10.1128/JB.183.15.4664-4667.2001.

30. Grass G, Otto M, Fricke B, Haney CJ, Rensing C, Nies DH, Munkelt D. 2005. FieF (YiiP) from *Escherichia coli* mediates decreased cellular accumulation of iron and relieves iron stress. Arch Microbiol 183:9–18. https://doi.org/10.1007/s00203-004-0739-4.

31. Lu M, Chai J, Fu D. 2009. Structural basis for autoregulation of the zinc transporter YiiP. Nat Struct Mol Biol 16:1063–1067. https://doi.org/10.1038/nsmb.1662.

32. Lu M, Fu D. 2007. Structure of the zinc transporter YiiP. Science 317:1746–1748. https://doi.org/10.1126/science.1143748.

33. Wei Y, Fu D. 2006. Binding and transport of metal ions at the dimer interface of the *Escherichia coli* metal transporter YiiP. J Biol Chem 281:23492–23502. https://doi.org/10.1074/jbc.M602254200.

34. Martin JE, Giedroc DP. 2016. Functional determinants of metal ion transport and selectivity in paralogous cation diffusion facilitator transporters CzcD and MntE in *Streptococcus pneumoniae*. J Bacteriol 198:1066–1076. https://doi.org/10.1128/JB.00975-15.

35. Hoch E, Lin W, Chai J, Hershfinkel M, Fu D, Sekler I. 2012. Histidine pairing at the metal transport site of mammalian ZnT transporters controls Zn^{2+} over Cd^{2+} selectivity. Proc Natl Acad Sci U S A 109:7202–7207. https://doi.org/10.1073/pnas.1200362109.

36. Montanini B, Blaudez D, Jeandroz S, Sanders D, Chalot M. 2007. Phylogenetic and functional analysis of the Cation Diffusion Facilitator (CDF) family: improved signature and prediction of substrate specificity. BMC Genomics 8:107. https://doi.org/10.1186/1471-2164-8-107.

37. Huang K, Wang D, Frederiksen RF, Rensing C, Olsen JE, Fresno AH. 2017. Investigation of the role of genes encoding zinc exporters *zntA*, *zitB*, and *fieF* during *Salmonella* Typhimurium infection. Front Microbiol 8:2656. https://doi.org/10.3389/fmicb.2017.02656.

38. Wei Y, Fu D. 2005. Selective metal binding to a membrane-embedded aspartate in the *Escherichia coli* metal transporter YiiP (FieF). J Biol Chem 280:33716–33724. https://doi.org/10.1074/jbc.M506107200.

39. Lisher JP, Higgins KA, Maroney MJ, Giedroc DP. 2013. Physical characterization of the manganese-sensing pneumococcal surface antigen repressor (PsaR) from *Streptococcus pneumoniae*. Biochemistry 52:7689–7701. https://doi.org/10.1021/bi401132w.

40. Eijkelkamp BA, Morey JR, Ween MP, Ong CY, McEwan AG, Paton JC, McDevitt CA. 2014. Extracellular zinc competitively inhibits manganese uptake and compromises oxidative stress management in *Streptococcus pneumoniae*. PLoS One 9:e89427. https://doi.org/10.1371/journal.pone.0089427.

41. McDevitt CA, Ogunniyi AD, Valkov E, Lawrence MC, Kobe B, McEwan AG, Paton JC. 2011. A molecular mechanism for bacterial susceptibility to zinc. PLoS Pathog 7:e1002357. https://doi.org/10.1371/journal.ppat.1002357.

42. Jacobsen FE, Kazmierczak KM, Lisher JP, Winkler ME, Giedroc DP. 2011. Interplay between manganese and zinc homeostasis in the human pathogen *Streptococcus pneumoniae*. Metallomics 3:38–41. https://doi.org/10.1039/c0mt00050g.

43. Outten CE, O'Halloran TV. 2001. Femtomolar sensitivity of metalloregulatory proteins controlling zinc homeostasis. Science 292:2488–2492. https://doi.org/10.1126/science.1060331.

44. Wang D, Hosteen O, Fierke CA. 2012. ZntR-mediated transcription of *zntA* responds to nanomolar intracellular free zinc. J Inorg Biochem 111:173–181. https://doi.org/10.1016/j.jinorgbio.2012.02.008.

45. Osman D, Martini MA, Foster AW, Chen J, Scott AJP, Morton RJ, Steed JW, Lurie-Luke E, Huggins TG, Lawrence AD, Deery E, Warren MJ, Chivers PT, Robinson NJ. 2019. Bacterial sensors define intracellular free energies for correct enzyme metalation. Nat Chem Biol 15:241–249. https://doi.org/10.1038/s41589-018-0211-4.

46. Patzer SI, Hantke K. 1998. The ZnuABC high-affinity zinc uptake system and its regulator Zur in *Escherichia coli*. Mol Microbiol 28:1199–1210. https://doi.org/10.1046/j.1365-2958.1998.00883.x.

47. Patzer SI, Hantke K. 2000. The zinc-responsive regulator Zur and its control of the *znu* gene cluster encoding the ZnuABC zinc uptake system in *Escherichia coli*. J Biol Chem 275:24321–24332. https://doi.org/10.1074/jbc.M001775200.

48. Campoy S, Jara M, Busquets N, Pérez De Rozas AM, Badiola I, Barbé J. 2002. Role of the high-affinity zinc uptake *znuABC* system in *Salmonella enterica* serovar Typhimurium virulence. Infect Immun 70:4721–4725. https://doi.org/10.1128/IAI.70.8.4721-4725.2002.

49. Beard SJ, Hashim R, Membrillo-Hernández J, Hughes MN, Poole RK. 1997. Zinc(II) tolerance in *Escherichia coli* K-12: evidence that the *zntA* gene (*o732*) encodes a cation transport ATPase. Mol Microbiol 25:883–891. https://doi.org/10.1111/j.1365-2958.1997.mmi518.x.

50. Brocklehurst KR, Hobman JL, Lawley B, Blank L, Marshall SJ, Brown NL, Morby AP. 1999. ZntR is a Zn(II)-responsive MerR-like transcriptional regulator of *zntA* in *Escherichia coli*. Mol Microbiol 31:893–902. https://doi.org/10.1046/j.1365-2958.1999.01229.x.

51. Grass G, Franke S, Taudte N, Nies DH, Kucharski LM, Maguire ME, Rensing C. 2005. The metal permease ZupT from *Escherichia coli* is a transporter with a broad substrate spectrum. J Bacteriol 187:1604–1611. https://doi.org/10.1128/JB.187.5.1604-1611.2005.

52. Karlinsey JE, Maguire ME, Becker LA, Crouch M-LV, Fang FC. 2010. The phage shock protein PspA facilitates divalent metal transport and is required for virulence of *Salmonella enterica* sv. Typhimurium. Mol Microbiol 78:669–685. https://doi.org/10.1111/j.1365-2958.2010.07357.x.

53. Raimunda D, Elso-Berberián G. 2014. Functional characterization of the CDF transporter SMc02724 (SmYiiP) in *Sinorhizobium meliloti*: roles in manganese homeostasis and nodulation. Biochim Biophys Acta 1838:3203–3211. https://doi.org/10.1016/j.bbamem.2014.09.005.

54. Cubillas C, Vinuesa P, Tabche ML, Dávalos A, Vázquez A, Hernández-Lucas I, Romero D, García-de los Santos A. 2014. The cation diffusion facilitator protein EmfA of *Rhizobium etli* belongs to a novel subfamily of Mn(2+)/Fe(2+) transporters conserved in α-proteobacteria. Metallomics 6:1808–1815. https://doi.org/10.1039/c4mt00135d.

55. Sun H, Xu G, Zhan H, Chen H, Sun Z, Tian B, Hua Y. 2010. Identification and evaluation of the role of the manganese efflux protein in *Deinococcus radiodurans*. BMC Microbiol 10:319. https://doi.org/10.1186/1471-2180-10-319.

56. Cubillas C, Vinuesa P, Tabche ML, García-de los Santos A. 2013. Phylogenomic analysis of Cation Diffusion Facilitator proteins uncovers Ni^{2+}/Co^{2+} transporters†. Metallomics 5:1634–1643. https://doi.org/10.1039/c3mt00204g.

57. Novichkov PS, Brettin TS, Novichkova ES, Dehal PS, Arkin AP, Dubchak I, Rodionov DA. 2012. RegPrecise web services interface: programmatic access to the transcriptional regulatory interactions in bacteria reconstructed by comparative genomics. Nucleic Acids Res 40:W604–W608. https://doi.org/10.1093/nar/gks562.

58. Dambach M, Sandoval M, Updegrove TB, Anantharaman V, Aravind L, Waters LS, Storz G. 2015. The ubiquitous *yybP-ykoY* riboswitch is a manganese-responsive regulatory element. Mol Cell 57:1099–1109. https://doi.org/10.1016/j.molcel.2015.01.035.

59. Thompson JD, Higgins DG, Gibson TJ. 1994. CLUSTAL W: improving the sensitivity of progressive multiple sequence alignment through sequence weighting, position-specific gap penalties and weight matrix choice. Nucleic Acids Res 22:4673–4680. https://doi.org/10.1093/nar/22.22.4673.

60. Datsenko KA, Wanner BL. 2000. One-step inactivation of chromosomal genes in *Escherichia coli* K-12 using PCR products. Proc Natl Acad Sci U S A 97:6640–6645. https://doi.org/10.1073/pnas.120163297.

61. Davis RW, Botstein D, Roth JR. 1982. Advanced bacterial genetics: a manual for genetic engineering. Cold Spring Harbor Laboratory, Cold Spring Harbor, NY.

62. Berggren RE, Wunderlich A, Ziegler E, Schleicher M, Duke RC, Looney D, Fang FC. 1995. HIV gp120-specific cell-mediated immune responses in mice after oral immunization with recombinant *Salmonella*. J Acquir Immune Defic Syndr Hum Retrovirol 10:489–495. https://doi.org/10.1097/00042560-199510050-00001.

63. Roldan RJ, Pajarillo AO, Greenberg JD, Karlinsey JE, Cafiero M, Frawley ER, Peterson LW. 2020. Propargylglycine-based antimicrobial compounds are targets of TolC-dependent efflux systems in *Escherichia coli*. Bioorg Med Chem Lett 30:126875. https://doi.org/10.1016/j.bmcl.2019.126875.

64. Will WR, Bale DH, Reid PJ, Libby SJ, Fang FC. 2014. Evolutionary expansion of a regulatory network by counter-silencing. Nat Commun 5:5270. https://doi.org/10.1038/ncomms6270.

65. Richardson AR, Payne EC, Younger N, Karlinsey JE, Thomas VC, Becker LA, Navarre WW, Castor ME, Libby SJ, Fang FC. 2011. Multiple Targets of Nitric Oxide in the Tricarboxylic Acid (TCA) Cycle of *Salmonella enterica* Serovar Typhimurium. Cell Host Microbe 10:33–43.